

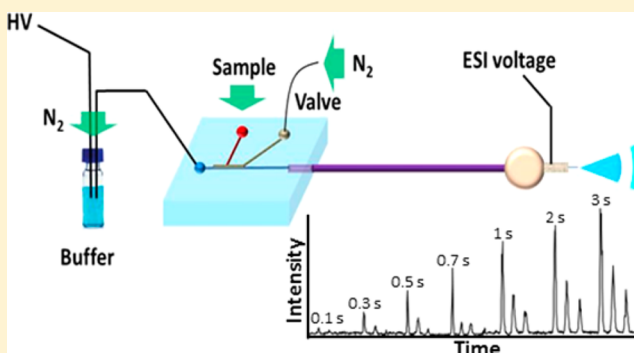
Pneumatic Microvalve-Based Hydrodynamic Sample Injection for High-Throughput, Quantitative Zone Electrophoresis in Capillaries

Ryan T. Kelly,^{*,†} Chenchen Wang,[‡] Sarah J. Rausch,[†] Cheng S. Lee,[‡] and Keqi Tang[§]

[†]Environmental Molecular Sciences Laboratory and [§]Biological Sciences Division, Pacific Northwest National Laboratory, P.O. Box 999, Richland, Washington 99352, United States

[‡]Department of Chemistry and Biochemistry, University of Maryland, College Park, Maryland 20742, United States

ABSTRACT: A hybrid microchip/capillary electrophoresis (CE) system was developed to allow unbiased and lossless sample loading and high-throughput repeated injections. This new hybrid CE system consists of a poly(dimethylsiloxane) (PDMS) microchip sample injector featuring a pneumatic microvalve that separates a sample introduction channel from a short sample loading channel, and a fused-silica capillary separation column that connects seamlessly to the sample loading channel. The sample introduction channel is pressurized such that when the pneumatic microvalve opens briefly, a variable-volume sample plug is introduced into the loading channel. A high voltage for CE separation is continuously applied across the loading channel and the fused-silica capillary separation column. Analytes are rapidly separated in the fused-silica capillary, and following separation, high-sensitivity MS detection is accomplished via a sheathless CE/ESI-MS interface. The performance evaluation of the complete CE/ESI-MS platform demonstrated that reproducible sample injection with well controlled sample plug volumes could be achieved by using the PDMS microchip injector. The absence of band broadening from microchip to capillary indicated a minimum dead volume at the junction. The capabilities of the new CE/ESI-MS platform in performing high-throughput and quantitative sample analyses were demonstrated by the repeated sample injection without interrupting an ongoing separation and a linear dependence of the total analyte ion abundance on the sample plug volume using a mixture of peptide standards. The separation efficiency of the new platform was also evaluated systematically at different sample injection times, flow rates, and CE separation voltages.



Electrospray ionization mass spectrometry (ESI-MS)-based proteomic and metabolomic analyses^{1,2} rely on chemical separations prior to ionization to add selectivity, reduce mass spectral congestion, and minimize ionization suppression at the electrospray source. Although liquid chromatography (LC) is the most widely used separation method for “omic” analyses, capillary electrophoresis (CE) has distinct advantages in the analysis of ultrasmall samples,³ including single cells,^{4–8} for which trace analytes can otherwise be lost on chromatographic media. CE is also advantageous for performing rapid, high-resolution separations, particularly in the microchip format.^{9–11}

The injection method used for CE analyses plays a major role in the overall separation performance in terms of quantitation, throughput, sensitivity, and resolution. For CE performed in fused-silica capillaries, the capillary inlet is transferred from the run buffer to a sample reservoir, and the sample is injected electrokinetically or hydrodynamically.¹² For electrokinetic injection, analytes migrate into the column under an applied electric field through a combination of electroosmotic flow and electromigration. For hydrodynamic injection, a pressure differential across the separation column is used to load a sample plug onto the column. Although electrokinetic injection enables simpler instrumentation and greater achievable enrichment

factors when used in combination with sample stacking techniques¹³ relative to hydrodynamic injection, it preferentially samples higher mobility ions and, thus, introduces a quantitative bias that must be carefully accounted for using calibration standards.¹² In contrast, hydrodynamic injection produces a sample plug that is representative of the original sample. For microchip-based CE injections, electrokinetic injection is generally used, although efforts to implement hydrodynamic injection for microfluidic separations have also been explored.^{14,15} For “gated” electrokinetic injections,¹⁶ sample is driven to a waste reservoir, and then voltages are adjusted to divert a portion of the sample into the separation channel for a given period of time before initiating the separation. The amount of sample loaded is proportional to the injection time. For “pinched” injections,¹⁷ voltages are arranged and switched such that only the sample present in the intersection is injected for separation. As with capillary-based electrokinetic injection, gated injection preferentially samples high-mobility analytes but can

Received: May 21, 2014

Accepted: May 27, 2014

Published: May 27, 2014

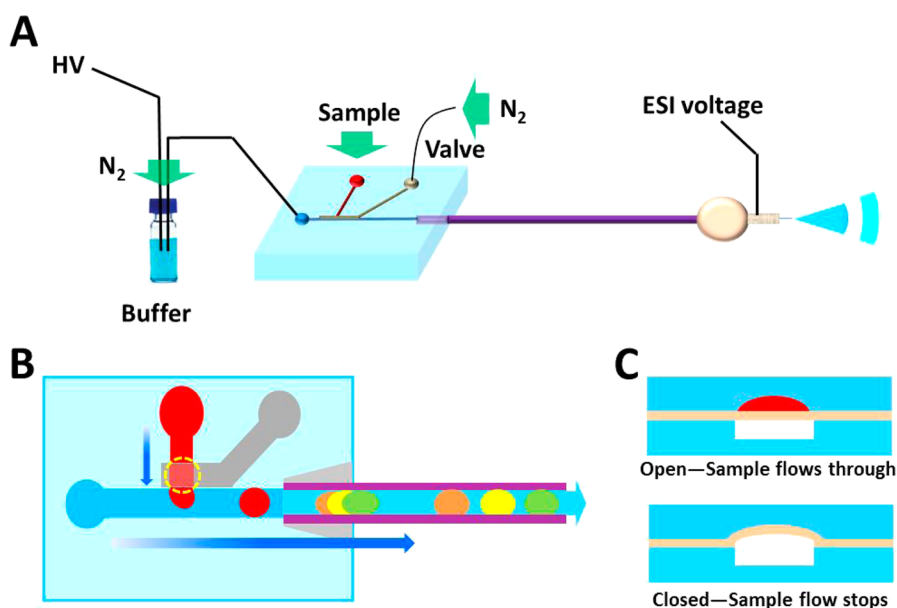


Figure 1. Device schematics. (A) Overview of the hybrid microchip/capillary CE–MS platform. (B) Depiction of sample injection upon valve actuation and subsequent electrophoretic separation. Voltage is continuously applied across the separation channel. Briefly opening the pneumatic valve hydrodynamically injects sample into the main channel for CE separation. (C) Side view of the flow (red) and control (white) channels separated by a membrane in open (top) and closed (bottom) states.

accommodate a range of sample volumes. In contrast, for pinched injections, the size of the injected sample plug is fixed by the intersection volume. Sampling biases are generally less pronounced for pinched injections but are also present as a result of the mobility-dependent rate of analyte depletion from the sample reservoir.

The sample injection process typically interrupts the electric field in the separation channel such that a separation in process must be completed prior to the commencement of a subsequent separation. This has implications for high-throughput measurements because the time prior to elution of the first analyte is essentially wasted and the overall duty cycle is reduced. In addition, multiplexed injection schemes based on the Hadamard or Fourier transform, which can substantially enhance detection sensitivity, are difficult to implement. These limitations have spurred development of alternative injection methods that increase duty cycle and avoid interrupting ongoing separations. For example, Imasaka and co-workers¹⁸ added sample to the run buffer and used a high-powered laser to photobleach all of the fluorescent analyte except during sample injection. The light was modulated in a pseudorandom sequence, and the Hadamard transform (HT) was applied to realize an ~ 8 -fold gain in S/N. The same group also implemented HT–CE for nonfluorescent analytes by electrokinetically injecting sample into the middle of a capillary through a laser-etched hole.¹⁹ In that implementation, the potentials applied for separation and injection had to be carefully balanced to minimize leakage of the run buffer into the large sample reservoir. Chiu et al.²⁰ developed a unique microfluidic device with an array of separation channels having different lengths that were loaded with sample simultaneously and combined into a single detection channel to implement Fourier transform CE. Price and Culbertson^{21,22} used an electroactive polymer at the injection cross of a microchip CE device to rapidly and repeatedly inject plugs of sample hydrodynamically into the separation channel while the rest of the sample was diverted to waste. In general, the ability to

perform repeated, overlapping injections comes with the trade-off of wasting the vast majority of the sample.

We recently developed a microfluidic CE platform²³ that employed a pneumatic microvalve, created using multilayer soft lithography,²⁴ at the intersection of a T-shaped channel to hydrodynamically inject sample into the separation channel. The separation voltage was continuously applied, and when the valve was briefly opened, a plug of sample was pressure-driven onto the separation channel. This simple approach enabled rapid and repeatable overlapping separations, eliminated analyte waste, and avoided the sampling biases inherent in electrokinetic injections. The device used poly(dimethylsiloxane) (PDMS) as a substrate because the elastomeric properties of PDMS were required for implementation of the pneumatic microvalve. Unfortunately, PDMS poses a challenge for high-resolution separations as a result of its propensity for analyte adsorption.²⁵ In addition, detection was limited to laser-induced fluorescence of the analytes due to difficulty in achieving stable and repeatable CE–MS analyses within monolithic PDMS devices.

Here, we report on a hybrid microchip/capillary device for CE–MS analysis of unlabeled peptides. A T-shaped PDMS microchannel with a pneumatic microvalve at the intersection is used for programmable hydrodynamic sample injection, but the microchannel interfaces with a 20-cm-long fused-silica capillary separation column immediately following the injection region. The separation column terminates at a sheathless electrospray interface for high-sensitivity detection of the separated analytes. The separation was operated in a pressure-assisted mode to provide a stable flow rate at the ESI source at flow rates ranging from 20 to 100 nL/min. The platform enables variable sample injection volumes, no quantitative bias, and repeated, programmable, overlapping separation for rapid optimization and high-throughput measurements. The technology is expected to facilitate the rapid analysis of large numbers of samples as well as multiplexed and multidimensional separations.

EXPERIMENTAL SECTION

Materials. Leucine enkephalin, kemptide, angiotensin II, methanol, acetic acid, hydrofluoric acid, ammonium acetate, and hydroxypropyl cellulose (HPC, average MW $\sim 100\,000$) were purchased from Sigma-Aldrich (St. Louis, MO). Water was purified using a Barnstead Nanopure Infinity system (Dubuque, IA). Peptide stock solutions were prepared individually in water at a concentration of 1 mg/mL. A 10 μM mixture of the three peptides was then prepared by dilution from the stock solutions into the run buffer. The run buffer was 9:1 of 0.1 M acetic acid in water/methanol. Colored dye was used as supplied by the manufacturer (ESCO Foods, Inc., San Francisco, CA) for visualizing pressure-driven injection and transfer of the sample plug to the capillary. Polydimethylsiloxane (PDMS) was purchased as Dow Corning Sylgard 184 from Ellsworth Adhesives (Germantown, WI). Fused-silica capillaries were from Polymicro Technologies (Phoenix, AZ), and acid enduring epoxy (EP42HT-2) was from Masterbond (Hackensack, NJ).

Microchip Design and Fabrication. A schematic of the hybrid microfluidic/capillary device is shown in Figure 1. The PDMS microchip was created from three patterned templates: a control layer, a flow layer and a cover plate, using multilayer soft lithography. Figure 2 shows an exploded view of the three aligned

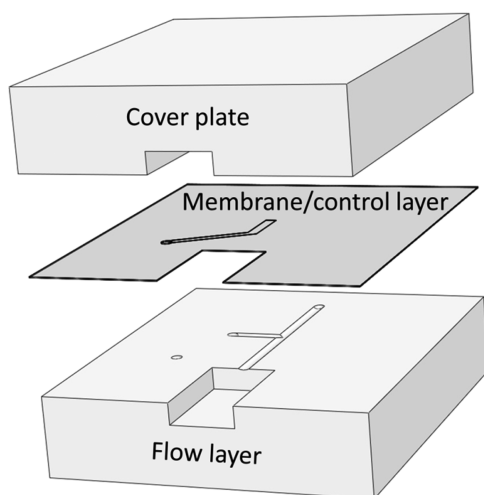


Figure 2. Exploded view of the three substrates comprising the microfluidic device.

PDMS substrates that comprised the microdevice. Template fabrication was similar to previous work.²⁶ The control layer channel was 25 μm tall and 100 μm wide and was rectangular in cross section. The flow layer channels were $\sim 10\,\mu\text{m}$ tall and 100 μm wide and were rounded in cross section to enable complete channel closure using the on-chip pneumatic valve.²⁴ To accommodate in-line insertion of a fused-silica capillary with the microchannel, the flow channel terminated at a channel that had a rectangular cross section, a height of 160 μm , and a width of 310 μm . The cover plate contained a channel of rectangular cross section that was 310 μm wide and 110 μm thick.

PDMS was prepared by thoroughly mixing Sylgard 184 base and curing agent at a 10:1 ratio. The PDMS was poured onto the control layer template and spin-coated at 2000 rpm for 30 s. PDMS was also poured over the flow layer and cover plate templates to a thickness of 3–4 mm and degassed under vacuum. All substrates were cured at 70 $^{\circ}\text{C}$ for 2 h. The flow layer substrate was then removed from its template, and holes were

formed using a 20-gauge catheter punch (Syneo, West Palm Beach, FL). Debris was removed from the substrate by applying compressed nitrogen, followed by Scotch Magic Tape (3M, St. Paul, MN) to both sides. The surfaces of the flow layer and control layer substrates were activated in an oxygen plasma system (PX-250, March Plasma Systems, Westlake, OH) at 50 W power and 200 mTorr pressure for 30 s. Following activation, the flow layer substrate was aligned at the sample introduction intersection and brought into contact with the control layer with the aid of a digital microscope (Keyence VHX-600, Osaka, Japan). The irreversibly bonded assembly was placed in an oven at 70 $^{\circ}\text{C}$ for 1 h to improve bond strength, and then the bonded flow and control substrates were cut and removed from the control layer template. It was necessary to remove the portion of the membrane that spanned the capillary insertion channel. This was accomplished by grasping the suspended membrane with a pair of fine-tipped tweezers and carefully pulling in such a way that the membrane tore along the channel walls. A hole was punched through both substrates as described above to provide access to the pneumatic valve, and the assembly was again cleaned using a combination of compressed nitrogen and Scotch tape. The microchip was completed by aligning and bonding the flow and control layers to the cover plate as described above.

Fused-Silica Capillary Preparation and Device Assembly

Fused-silica capillaries having an o.d. of 140 μm and an i.d. of 30 μm were passivated with HPC to suppress electroosmotic flow. The coating was prepared by first flushing the fused-silica capillary with 1 mL of 1 M HCL solution, followed by flushing the capillary with 200 μL of 5% HPC in water. The capillary was then flushed with deionized water to remove excess HPC. The treated capillary was subsequently cut into equal lengths, and $\sim 3\,\text{cm}$ at the end of each length was chemically etched in 49% HF to render it porous for electrical contact as described previously.²⁷ The etching of capillaries took place in bundles with each batch providing ~ 10 capillaries using an approach adapted from previous work.²⁸ Note that HF is extremely corrosive, and its use requires at a minimum a fume hood, goggles, rubber gloves, and an apron. The distal end (inlet) of the capillary was then sheathed using an $\sim 5\,\text{cm}$ length of 360- μm -o.d., 150- μm -i.d. capillary and sealed in place with epoxy to provide easy assembly and better size matching with the microfluidic device. This sheathed end was cut a few mm from the inlet using a dicing saw (SYJ-400, MTI Corp., Richmond, CA) to provide a clean interface at the microchip–capillary transition. Alternatively, a 360- μm -o.d., 30- μm -i.d. capillary can be used for separation, rendering the sheath capillary unnecessary, but the etching time will be much longer. The porous emitter was housed in a metal tube through a PEEK tee (Upchurch Scientific, Oak Harbor, WA) (Figure 1A) as described in our previous work.²⁷ The emitter end of the etched capillary protruded 1–2 mm from the metal tube. The capillary inlet end was then inserted under a microscope into the 3 mm-long capillary-accepting channel on the microchip, and a small amount of PDMS was applied at the microchannel–capillary interface. The PDMS was cured by placing the assembly in an oven at 110 $^{\circ}\text{C}$ for 20 min.

Device Operation. The controller and software interface for the microfluidic valve have been described previously.^{23,26} The tygon tubing used to connect the valve controller to the on-chip valves was filled with water, and a pressure of 20 psi was applied to purge all air from the microvalves, thus preventing the introduction of bubbles into the flow channels.²³ With the valve closed, a few microliters of sample was loaded into a pipet tip (part no. 37001-150, VWR, Radnor, PA), which was then press-

fitted into the sample port on the chip. To pressurize the sample, a length of tubing connected to a digital pressure controller (PCD-100PSIG-D-IPC-PCV10, Alicat Scientific, Tucson, AZ) was inserted into a round PDMS plug, which was in turn pressed into the wide end of the pipet tip to form an airtight seal. The sample was pressurized to 5 psi to dead-end-fill the sample against the closed valve, and then the sample pressure was adjusted as needed for operation. The CE run buffer was loaded into a sample vial that was then sealed to allow a N_2 back pressure to be applied to the buffer liquid, as shown in Figure 1A. High voltage for CE operation was applied to a platinum wire inserted into the buffer solution using a Glassman High Voltage power supply (High Bridge, N. J.). A transfer fused-silica capillary (360 μm o.d., 50 μm i.d.) with one end inserted into the buffer solution and the other end press-fitted into the microfluidic chip using a short length of Tygon sheath tubing was used to provide the CE run buffer to the device.²⁹ The N_2 back pressure controlling the flow through the CE capillary, referred to as the eluting pressure, was regulated using a second digital pressure controller (Alicat Scientific). A second voltage of ~ 2 kV was applied to the metal tube at the capillary outlet through a Bertan power supply (Hauppauge, N. Y.) for stable electrospray operation.

MS Operation and Data Processing. All CE-nanoESI-MS analyses were performed using a triple quadrupole mass spectrometer (TSQ Quantum Ultra, Thermo Fisher Scientific, Waltham, MA). The inlet capillary of the mass spectrometer was maintained at 200 $^{\circ}\text{C}$. Mass spectra were acquired in full scan mode covering an m/z range from 300 to 1000 at an acquisition rate of 2 Hz. For data analysis, the raw MS files were processed using Thermo Xcalibur Qual Browser 2.2. Extracted ion electropherograms were obtained using m/z ranges of 386–388, 524–526, and 555.5–557.5 for kemptide, angiotensin II, and leucine enkephalin, respectively. The resulting electropherograms were exported to Microsoft Excel for further processing.

RESULTS AND DISCUSSION

The microfluidic portion of the platform comprises a simple tee channel with a “push-up” microvalve³⁰ at the intersection that separates the sample injection channel from the separation channel. This arrangement offers several advantages over common injection strategies for both microfluidic and capillary-based CE. CE in capillaries requires the capillary inlet to be physically transferred between sample and run buffer reservoirs for either pressure-based or electrokinetic injection. This can reduce measurement throughput and makes the injection of very narrow bands difficult. Microchip CE using gated injection enables variable sample loading based on injection time, but with a strong quantitative bias (as with capillary-based electrokinetic injection). Pinched microfluidic injection enables the formation of very narrow sample plugs for fast, efficient separations, but the injected volume is fixed by the device geometry, and a quantitative bias may still be present because of more rapid depletion of high-mobility species from the sample reservoir. In contrast, our injector allows the separation voltage to be continuously applied and a variable-volume sample plug to be injected without interrupting an ongoing separation, thus enabling higher throughput and rapid optimization of the separation conditions.

Device fabrication was largely straightforward using multilayer soft lithography. Fabrication utilized three different patterned templates to create the flow, control, and cover plate layers, and the flow layer comprised two aligned and separately patterned lithography steps. All layers were created from a single

photomask using a previously described approach,³¹ which substantially reduced the time and cost required for glass photomask production. To insert the capillaries in-line with the microchannel and provide a seamless transition from microchannel to capillary, it was necessary to remove the membrane that spanned the insertion channel. This was performed using fine-tipped tweezers and had variable results. When the membrane tore cleanly at the microchannel–capillary interface, a leak-free junction could be formed by simply pressing the capillary firmly against the microchannel inlet such that the PDMS material served as a gasket for the capillary end. Otherwise, it was necessary to introduce uncured PDMS around the capillary and then cure at elevated temperature. The latter approach became the default procedure to avoid needing to test each device for leaks.

A pressure-driven injection sequence is shown in Figure 3 using an aqueous dye in place of the sample and in the absence of



Figure 3. Photomicrographs showing a pressure-driven injection sequence. Additional description is in the text.

an electric field. The eluting and sample pressures were 2.0 and 2.5 psi, respectively, and the valve opening time was 65 ms. The interfaced capillary had an i.d. of 30 μm and was 75 mm long. To estimate the volume of this and other sample plugs, it was necessary to know the cross-sectional area of the rounded microchannel. This was determined by filling the separation channel in both the microchip and capillary with perfluorodecalin, an immiscible oil, injecting colored dye from the sample channel, and comparing the length of the plug in the microchannel and inside the capillary of known diameter. It was determined that the microchannel had a cross-sectional area of 450 μm^2 , equivalent to a 24- μm -diameter capillary. The injection volume shown in Figure 3 was approximately 400 pL, a plug size typical of microchip electrophoresis, and the volume could easily be tuned larger or smaller by adjusting the valve opening time and the sample injection pressure. For the eluting pressures evaluated here, the flow rate was found to range from ~ 20 to 100 nL/min, calculated by the migrating velocity of the

dye plug. These flow rates are in the nanoflow regime, enabling high ionization efficiency for improved MS detection.³²

The number of theoretical plates was evaluated as a function of separation potential for initial characterization of the hybrid CE separation and was calculated using the formula

$$N = 16 \left(\frac{t_r}{w} \right)^2$$

where t_r is the retention time and w is the baseline peak width. As expected, the plate number increases linearly with the voltage, as shown in Figure 4, albeit with a y -intercept offset from the origin

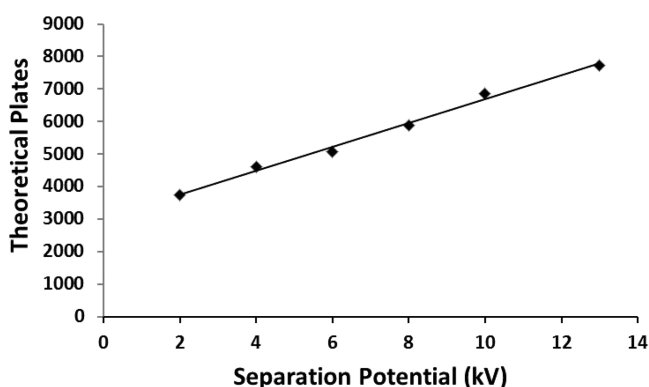


Figure 4. Theoretical plates for leucine enkephalin as a function of separation potential. For each separation, the injection and elution pressures were 2 psi and the injection time was 500 ms.

resulting from the pressure-assisted mode of separation. Further increasing the separation potential above 13 kV in an attempt to increase separation efficiency resulted in occasional electrical breakdown in the channels in our current setup, so 13 kV was used as the optimal operating parameter for subsequent experiments to achieve reproducible and safe operation.

The computer-controlled, pressure-driven injection method described here enables significant flexibility and easy tuning of separation conditions, as well as rapid and automated acquisition of those separations. As an example, Figure 5 shows a continuous separation of repeated injections of a three-peptide mixture containing kemptide, angiotensin II and leucine enkephalin. During this experiment, the valve was opened every 1.25 min to inject the sample, and the valve opening time was varied from 0.1 to 3 s throughout the series. The trend of increasing peak intensity with injection time is clear and linear, indicating leak-

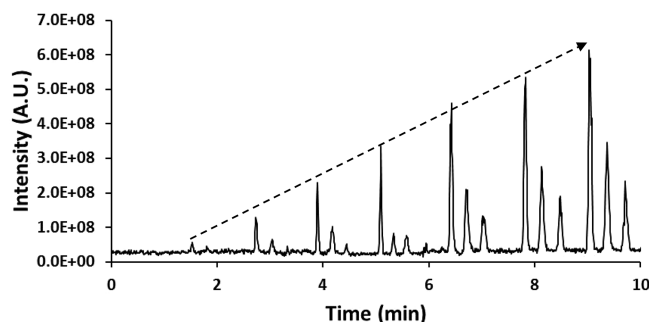


Figure 5. Automated, repeated injections of sample mixture containing kemptide, angiotensin II, and leucine enkephalin (in order of highest to lowest mobility) with fixed interval of 1.25 min. Sample injection times from left to right were 0.1, 0.3, 0.5, 0.7, 1.0, 2.0, and 3.0 s.

free, accurate and rapid sample injection through the pneumatic valve based microchip. The capability for uninterrupted acquisition of repeated separations under different conditions provides straightforward manipulation for experiment operation in aspects of system optimization and automation. In addition, in contrast to common injection techniques that send the vast majority of sample to waste to accomplish an efficient injection or require a large sample reservoir, our approach enables a minimum volume (a few microliters in the present work) of sample to be loaded by pipet onto the device and for that entire sample to be used for repeated injections. This will be useful for multiplexed separations to improve signal-to-noise ratio and for the analysis of precious biological samples.

The trade-off between separation efficiency and S/N as the injection volume is varied is shown in Figure 6. In part A, the number of theoretical plates as a function of injection time is shown for three different elution pressures. Values were

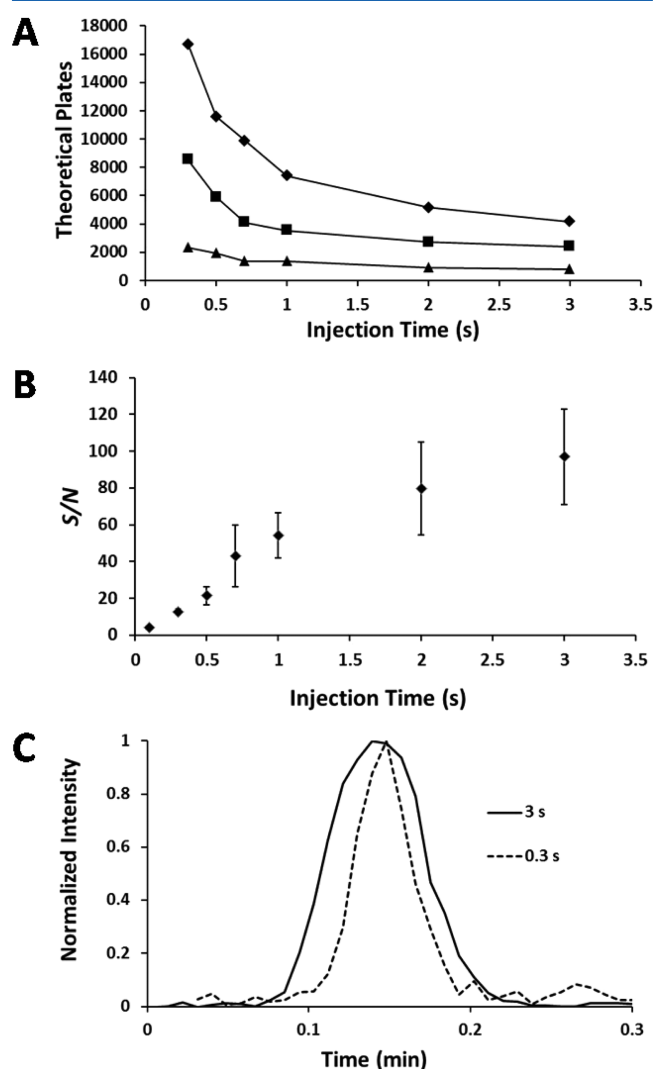


Figure 6. Separation performance as a function of eluting pressure and injection time. (A) Theoretical plates vs injection time for leucine enkephalin. Separation potential was 13 kV for each separation. The eluting and injection pressures were both 1 (◆), 2 (■), and 4 psi (▲). (B) S/N vs injection time for kemptide. The eluting and injection pressures were both 2 psi. Error bars are standard deviation for three replicate separations. (C) Kemptide peak resulting from 0.3 and 3 s injections (2 psi eluting and injection pressures).

calculated for the leucine enkephalin peak. Higher flow rates resulted in reduced plate counts due to increased Taylor dispersion, and in each case, smaller injection plugs produced narrower detected peaks and, thus, greater plate counts. The modest separation efficiency achieved here is due to the pressure-assisted mode of operation, as even at the lowest pressure used (1 psi providing a flow rate of ~ 20 nL/min), Taylor dispersion degraded separation performance. We will explore alternative strategies, such as the CITEP-based sample stacking/separation, to counterbalance Taylor dispersion²⁷ or the recently developed electrokinetically driven sheath-flow interface^{3,33} to achieve high-resolution CE–MS separations and avoid the pressure-driven flow used here. Although plate count diminished with increasing injection times, the S/N showed the opposite trend, increasing with longer injections. Part B shows the S/N for kemptide for three replicate measurements using 2 psi for both the sample injection and the elution pressure. Noise was calculated from the data points in the range of 0.4–0.2 min before the apex of each peak. Part C shows two overlaid kemptide peaks normalized to 100% intensity, one acquired from a 0.3 s injection, and the other, from a 3 s injection. The peak resulting from a 0.3 s injection is clearly narrower than that from the 3 s injection, but the S/N is also substantially reduced, as reflected in the baseline adjacent to the peak, which is expected for lower sample loading amounts under nonstacking separation conditions.

In addition to the ability to perform repeated, waste-free, programmable injections without impacting ongoing separations, another key benefit of the platform is that sample injection is pressure-based and expected to avoid quantitative biases inherent in electrokinetic injection strategies. We verified this by evaluating the peak area for each of the peptides in the mixture for injection times ranging from 0.3 to 7 s under constant pressure. As shown in Figure 7, the peak area for each analyte

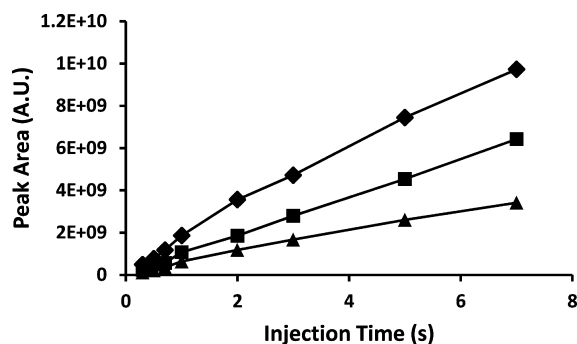


Figure 7. Peak areas for kemptide (◆), angiotensin II (■), and leucine enkephalin (▲) as a function of injection time.

increases linearly with injection time, and as such, the proportionality between peptides is maintained, even across this range of injection times spanning more than a factor of 20.

CONCLUSIONS AND OUTLOOK

We have demonstrated a microfluidic valve-based pressure injector for use with capillary-based CE–MS analyses. The computer-controlled pneumatic microvalve enables volumes ranging from picoliters to nanoliters to be injected based on valve opening time and injection pressure, and a seamless interface from microchannel to capillary prevents sample losses and large dead volumes. None of the sample is wasted in the injection process, and the remaining sample can be injected repeatedly under different conditions (e.g., injection times) for rapid

optimization of the analysis and potentially for improved detection by multiplexing. Because the injection is pressure-based, no quantitative bias is observed. The ability to rapidly inject a sample without interrupting an ongoing separation has implications for high-throughput analyses because the otherwise wasted time prior to elution of the first peak can be effectively utilized. Although only a single valve was employed here, this work opens the door for the powerful sample handling capabilities of multilayer soft lithography to be applied to CE analyses. For example, on-column sample derivatization³⁴ will be feasible by simultaneously opening opposing valves containing sample and label.²⁶ In addition, multiplexed valving strategies³⁰ enable a large number of input channels to be addressed using a modest number of valves (e.g., 128 inputs controlled with 14 valves). Adapting this approach to CE will enable the high-throughput analysis of large numbers of samples for, e.g., measurement of prefractionated samples from an orthogonal separation.

AUTHOR INFORMATION

Corresponding Author

*E-mail: ryan.kelly@pnnl.gov.

Notes

The authors declare no competing financial interest.

ACKNOWLEDGMENTS

We thank Brandon Kelly for assistance with microfluidic device fabrication. The research described in this paper was conducted under the Laboratory Directed Research and Development Program at Pacific Northwest National Laboratory (PNNL), a multiprogram national laboratory operated by Battelle for the U.S. Department of Energy, and grants from the NIH National Cancer Institute (1R33CA155252 and R21 CA143177). The research was performed using EMSL, a national scientific user facility sponsored by the Department of Energy's Office of Biological and Environmental Research and located at PNNL.

REFERENCES

- (1) Angel, T. E.; Aryal, U. K.; Hengel, S. M.; Baker, E. S.; Kelly, R. T.; Robinson, E. W.; Smith, R. D. *Chem. Soc. Rev.* **2012**, *41*, 3912–3928.
- (2) Gika, H. G.; Theodoridis, G. A.; Plumb, R. S.; Wilson, I. D. *J. Pharm. Biomed. Anal.* **2014**, *87*, 12–25.
- (3) Sun, L. L.; Zhu, G. J.; Zhao, Y. M.; Yan, X. J.; Mou, S.; Dovichi, N. J. *Angew. Chem., Int. Ed.* **2013**, *52*, 13661–13664.
- (4) Hofstadler, S. A.; Severs, J. C.; Smith, R. D.; Swanek, F. D.; Ewing, A. G. *Rapid Commun. Mass Spectrom.* **1996**, *10*, 919–922.
- (5) Stuart, J. N.; Sweedler, J. V. *Anal. Bioanal. Chem.* **2003**, *375*, 28–29.
- (6) Woods, L. A.; Roddy, T. P.; Ewing, A. G. *Electrophoresis* **2004**, *25*, 1181–1187.
- (7) Xiao, Y. X.; Feng, Y. P.; Da, S. L.; Yeung, E. S. *Prog. Chem.* **2004**, *16*, 543–553.
- (8) Huang, W.-H.; Ai, F.; Wang, Z.-L.; Cheng, J.-K. *J. Chromatogr., B* **2008**, *866*, 104–122.
- (9) Jacobson, S. C.; Culbertson, C. T.; Daler, J. E.; Ramsey, J. M. *Anal. Chem.* **1998**, *70*, 3476–3480.
- (10) Fritzsche, S.; Hoffmann, P.; Belder, D. *Lab Chip* **2010**, *10*, 1227–1230.
- (11) Henley, W. H.; Ramsey, J. M. *Electrophoresis* **2012**, *33*, 2718–2724.
- (12) Breadmore, M. C. *Bioanalysis* **2009**, *1*, 889–894.
- (13) Osbourn, D. M.; Weiss, D. J.; Lunte, C. E. *Electrophoresis* **2000**, *21*, 2768–2779.
- (14) Karlinsey, J. M. *Anal. Chim. Acta* **2012**, *725*, 1–13.
- (15) Saito, R. M.; Coltro, W. K. T.; de Jesus, D. P. *Electrophoresis* **2012**, *33*, 2614–2623.

- (16) Harrison, D. J.; Manz, A.; Fan, Z.; Lüdi, H.; Widmer, H. M. *Anal. Chem.* **1992**, *64*, 1926–1932.
- (17) Jacobson, S. C.; Hergenroder, R.; Koutny, L. B.; Warmack, R. J.; Ramsey, J. M. *Anal. Chem.* **1994**, *66*, 1107–1113.
- (18) Kaneta, T.; Yamaguchi, Y.; Imasaka, T. *Anal. Chem.* **1999**, *71*, 5444–5446.
- (19) Hata, K.; Kaneta, T.; Imasaka, T. *Anal. Chem.* **2004**, *76*, 4421–4425.
- (20) Allen, P. B.; Doepker, B. R.; Chiu, D. T. *Anal. Chem.* **2007**, *79*, 6807–6815.
- (21) Price, A. K.; Anderson, K. M.; Culbertson, C. T. *Lab Chip* **2009**, *9*, 2076–2084.
- (22) Price, A. K.; Culbertson, C. T. *Anal. Chem.* **2009**, *81*, 8942–8948.
- (23) Sun, X. F.; Kelly, R. T.; Danielson, W. F.; Agrawal, N.; Tang, K. Q.; Smith, R. D. *Electrophoresis* **2011**, *32*, 1610–1618.
- (24) Unger, M. A.; Chou, H. P.; Thorsen, T.; Scherer, A.; Quake, S. R. *Science* **2000**, *288*, 113–116.
- (25) Ocvirk, G.; Munroe, M.; Tang, T.; Oleschuk, R.; Westra, K.; Harrison, D. J. *Electrophoresis* **2000**, *21*, 107–115.
- (26) Sun, X. F.; Tang, K. Q.; Smith, R. D.; Kelly, R. T. *Microfluid. Nanofluid.* **2013**, *15*, 117–126.
- (27) Wang, C. C.; Lee, C. S.; Smith, R. D.; Tang, K. Q. *Anal. Chem.* **2013**, *85*, 7308–7315.
- (28) Kelly, R. T.; Page, J. S.; Tang, K.; Smith, R. D. *Anal. Chem.* **2007**, *79*, 4192–4198.
- (29) Kelly, R. T.; Tang, K.; Irimia, D.; Toner, M.; Smith, R. D. *Anal. Chem.* **2008**, *80*, 3824–3831.
- (30) Melin, J.; Quake, S. R. *Annu. Rev. Biophys. Biomol. Struct.* **2007**, *213*–231.
- (31) Kelly, R. T.; Sheen, A. M.; Jambovane, S. *RSC Adv.* **2013**, *3*, 20138–20142.
- (32) Wilm, M.; Mann, M. *Anal. Chem.* **1996**, *68*, 1–8.
- (33) Wojcik, R.; Dada, O. O.; Sadilek, M.; Dovichi, N. J. *Rapid Commun. Mass Spectrom.* **2010**, *24*, 2554–2560.
- (34) Underberg, W. J. M.; Waterval, J. C. M. *Electrophoresis* **2002**, *23*, 3922–3933.